Preemission cluster energies in preequilibrium nuclear reactions

Chinmay Basu* and Sudip Ghosh†
Saha Institute of Nuclear Physics, 1/AF Bidhan Nagar, Calcutta 700 064, India
(Received 31 October 1996)

A formalism is developed to evaluate the energy distribution of light clusters inside an excited nucleus. Its importance in predicting emitted cluster spectra is demonstrated by comparison with experiment and other models. [S0556-2813(97)05411-3]

PACS number(s): 24.10.Cn, 21.60.Gx, 23.60.+e, 23.70.+j

I. INTRODUCTION

Preequilibrium (PEQ) emission of clusters has turned out much more difficult to solve than nucleon emission. The problem lies in evaluating the cluster formation probability and its energy distribution inside the excited mother nucleus. A number of methods, with and without adjustable parameters, are used for evaluating the cluster formation probability but the role of its preemission energy distribution is ignored in all PEQ reaction studies, both quantum mechanical and semiclassical. For cluster emissions, the quantum-mechanical Feshbach-Kerman-Koonin (FKK) theory has so far been applied to α particles only. It assumes that the cluster formed in the ground state of the target is emitted by the single-step knockout mechanism [1]. The evaluation of preemission cluster energy distributions is therefore irrelevant.

The semiclassical exciton model has been used more widely to investigate deuteron, triton, helion, and α-particle PEQ spectra (see [2] and references therein), but with mixed success. It usually reproduces the α-particle spectra fairly well and sometimes the triton spectra also, but grossly underpredicts the high-energy part of deuteron and helion spectra [3–5]. A possible reason for this partial failure of the exciton model may lie in its implicit assumption that every configuration of each intermediate state occurs with equal *a priori* probability during the equilibration process. In this context, the energy distribution of the cluster prior to its emission assumes fundamental importance. In this work we develop a simple formalism for evaluating this energy distribution and show its importance in predicting emitted cluster spectra in PEQ reactions.

Of the two well-known PEQ reaction models, viz., the hybrid and exciton models, the former requires the explicit evaluation of preemission ejectile energy distribution. The hybrid model in its present version, however, is valid for nucleon emissions only. We extend it to cluster emissions as well. In order to clarify this extension, we begin Sec. II with a brief outline of the basic features of the model for PEQ nucleon emissions, which is followed by the development of the model for cluster emissions. In Sec. III we compare the results of the extended hybrid model with those of the exciton model and experiment. The relevance of the evaluation of preemission energy distribution is discussed in Sec. IV.

*Electronic address: chinmay@hp1.saha.ernet.in
†Electronic address: sudip@hp1.saha.ernet.in

II. THE HYBRID MODEL FOR CLUSTERS EMISSIONS

The hybrid model angle-integrated cross section for ejectile x with energy ϵ_x is given by [6] as

$$\sigma(\epsilon_x)=\sigma_{abs}\sum_{\substack{n=n_0\\ \Delta n=2}}^{\overline{n}} D_n W_n(\epsilon_x)\tau_n(\epsilon_x), \tag{1}$$

where σ_{abs} is the projectile absorption cross section, D_n the n-exciton state depletion factor, $W_n(\epsilon_x)$ the emission rate of x with energy ϵ_x from the n-exciton state, and $\tau_n(\epsilon_x)$ the mean lifetime of that particular configuration of the n-exciton state from which the emission occurs. The emission rate is expressed as

$$W_n(\epsilon_x)=f_n^x(E_x)\lambda_e(\epsilon_x), \tag{2}$$

where $f_n^x(E_x)$ is the preemission energy distribution of the ejectile, i.e., the number of x-type ejectiles in the n-exciton state with energy E_x measured from the Fermi energy ϵ_F ($E_x=\epsilon_x+B_x$, B_x being the ejectile separation energy). $\lambda_e(\epsilon_x)$ is the decay rate of this particular configuration of the n-exciton state where the ejectile has energy E_x.

Since the hybrid model looks at emissions from a particular configuration of the n-exciton state, the decay rate is calculated from the principle of detailed balance with the initial-state density as the single-particle level density g_x of the ejectile and the final-state density as that arising from the translational motion of the ejectile after emission [6]

$$\lambda_e(\epsilon_x)=\frac{(2s_x+1)\mu_x\epsilon_x\sigma_{inv}(\epsilon_x)}{\pi^2\hbar^3 g_x} \tag{3}$$

in terms of the intrinsic spin s_x, reduced mass μ_x, and inverse cross section $\sigma_{inv}(\epsilon_x)$.

The mean lifetime is then given by

$$\tau_n(\epsilon_x)=\frac{1}{\lambda_e(\epsilon_x)+\dfrac{2W}{\hbar}}, \tag{4}$$

where $2W/\hbar$ is the two-body interaction rate of the ejectile with the other nucleons of the system, W being the imaginary part of the optical model potential of the ejectile and the residual nucleus. Other methods of evaluating the two-body interaction rate are described in Ref. [6].

For nucleon emissions, g_x in Eq. (3) is the nucleon single-particle level density and $f_n^x(E_x)$ is written as [6]

$$f_n^x(E_x)=X_n^x P_n(E_x)=X_n^x\frac{\rho_n(U,E_x)}{\int_0^{E_c}\rho_n(U,E_x)dE_x}, \tag{5}$$

where X_n^x is the number of excited x-type nucleons in the n-exciton state. $P_n(E_x)$ is probability of the x-type nucleon having energy E_x inside the nucleus. It is assumed to be proportional to $\rho_n(U,E_x)$, the density of states in the n-exciton state when the nucleon has energy E_x and the remaining $(n-1)$ excitons share the residual energy $U=E_c-E_x$, where E_c is the excitation energy of the nucleus. The denominator in Eq. (5) is equal to $\rho_n(E_c)$, the density of states of the n-exciton state with excitation energy E_c. It is obtained straightforwardly from the normalization condition $\int_0^{E_c}P_n(E_x)dE_x=1$ so that the number X_n^x is conserved.

The problem of using Eq. (1) for cluster emissions lies in evaluating $f_n^x(E_x)$ of Eq. (2). While X_n^x, and hence $f_n^x(E_x)$ as well, is adequately defined for nucleons [6], no prescription is available for evaluating $f_n^x(E_x)$ for clusters. This requires the evaluation of the number of x-type clusters formed in the n-exciton state as well as their energy distribution prior to emission. We address these problems in the following subsections.

A. Number of clusters formed

Following Refs. [2,4,5,7], we consider that the x cluster can be formed in the (Z,N,A) nucleus through the coalescence of l excited nucleons and m nucleons from below the Fermi sea. For a cluster with x_π protons and x_ν neutrons $(x_\pi+x_\nu=A_x)$, $x_{\pi l}$ protons and $x_{\nu l}$ neutrons are selected from the p excited particles of the n-exciton state and $x_{\pi m}$ protons and $x_{\nu m}$ neutrons from the $A-p$ nucleons that are below the Fermi sea. We then have

$$x_\pi=x_{\pi l}+x_{\pi m},\quad x_\nu=x_{\nu l}+x_{\nu m}, \tag{6}$$

$$l=x_{\pi l}+x_{\nu l},\quad m=x_{\pi m}+x_{\nu m}. \tag{7}$$

The number of x clusters formed in the n-exciton state with energy E_x (measured from the Fermi energy ϵ_F) is

$$f_n^x(E_x)=\sum_{l=0}^{A_x} f_{nlm}^x(E_x),$$

$$f_{nlm}^x(E_x)=N_n^{lm}(x)\mathcal{P}_n^{lm}(E_x)=N_n^{lm}(x)K_n^{lm}(E_x)P_n^{lm}(E_x), \tag{8}$$

where $N_n^{lm}(x)$ is the number of x clusters that can be counted from the A nucleons under the constraints imposed by Eqs. (6) and (7). $\mathcal{P}_n^{lm}(E_x)$ is the cluster formation probability with energy E_x. This is factorized as the product of two independent probabilities $K_n^{lm}(E_x)$, the probability of the cluster nucleons being bound at the preassigned energy E_x, and $P_n^{lm}(E_x)$, the probability of the cluster having this energy E_x. In order to evaluate $f_n^x(E_x)$ two constraints are to be taken into account. These are the conservation of (a) the number of excited particles p and (b) the excitation energy while evaluating $N_n^{lm}(x)$ and $P_n^{lm}(E_x)$, respectively.

The conservation of p requires that

$$\sum_x\sum_l lN_n^{lm}(x)=p, \tag{9}$$

where the second summation is over all types of clusters. To simplify the evaluation of $N_n^{lm}(x)$ so that Eq. (9) is satisfied we write

$$N_n^{lm}(x)=\frac{pn_n^{lm}(x)}{\sum_x\sum_l ln_n^{lm}(x)}, \tag{10}$$

where $n_n^{lm}(x)$ is the number of x-type clusters that can be counted from A nucleons without the constraint of conserving p.

In the n-exciton state with p excited particles and h holes there can be $p-p_a+1$ different configurations when the projectile is made up of p_a nucleons. Each configuration, designated as j, is characterized by differnt numbers of excited protons $p_{\pi j}$, neutrons $p_{\nu j}$, proton holes $h_{\pi j}$, and neutron holes $h_{\nu j}$ $(p_{\pi j}+p_{\nu j}=p,\ h_{\pi j}+h_{\nu j}=h)$. It can be shown from induction that if a_π be the number of protons in the projectile, then $p_{\pi j}=a_\pi+j$, $h_{\pi j}=j$ and $p_{\nu j}=p-p_{\pi j}$, $h_{\nu j}=h-h_{\pi j}$, with $j=0,1,\ldots,p-p_a$.

For a given configuration j, the $x_{\pi l}$ and $x_{\pi m}$ protons constituting x_π are selected, respectively, from $p_{\pi j}$ excited protons and $Z-p_{\pi j}$ protons below the Fermi sea. Similarly, the $x_{\nu l}$ and $x_{\nu m}$ neutrons that go into x_ν are obtained from $p_{\nu j}$ and $N-p_{\nu j}$, respectively. Clearly, the number of x-type clusters that can be constituted from p excited particles and $A-p$ nucleons below the Fermi sea is the minimum of the ratios $p_{\pi j}/x_{\pi l}$, $p_{\nu j}/x_{\nu l}$, $(Z-p_{\pi j})/x_{\pi m}$, and $(N-p_{\nu j})/x_{\nu m}$.

Again, in the jth configuration, the x-type cluster may be constituted through different combinations of $x_{\pi l}$, $x_{\nu l}$, $x_{\pi m}$, and $x_{\nu m}$ as is evident from Eq. (6). Assigning $R(x_{\pi l},j)$ as the probability of a particular combination of $x_{\pi l}$, $x_{\nu l}$, $x_{\pi m}$, and $x_{\nu m}$ at a given j and ω_j as the statistical weight factor for the particular j, $n_n^{lm}(x)$ is expressed as

$$n_n^{lm}(x)=\sum_{j=0}^{p-p_a} w_j\sum_{\{x_{\pi l}\}}\left[\frac{p_{\pi j}}{x_{\pi l}},\frac{p_{\nu j}}{x_{\nu l}},\frac{Z-p_{\pi j}}{x_{\pi m}},\frac{N-p_{\nu j}}{x_{\nu m}}\right]_{min}R(x_{\pi l},j). \tag{11}$$

The summation $\{x_{\pi l}\}$ in Eq. (11) is over those values of $x_{\pi l}$, $x_{\nu l}$, $x_{\pi m}$, and $x_{\nu m}$ that satisfy both constraints (6) and (7).

Following [8],

$$R(x_{\pi l},j)=\frac{\binom{p_{\pi j}}{x_{\pi l}}\binom{p_{\nu j}}{x_{\nu l}}\binom{Z-p_{\pi j}}{x_{\pi m}}\binom{N-p_{\nu j}}{x_{\nu m}}}{\binom{p}{l}\binom{A-p}{m}}, \tag{12}$$

where $\binom{a}{b}=a!/(a-b)!b!$. The denominator is obtained by summing the numerator over those values of $x_{\pi l}$, $x_{\nu l}$, $x_{\pi m}$,

and $x_{\nu m}$ that satisfy constraint (7) alone with Eq. (6) remaining inoperative. The statistical weight factor ω_j is written as a binomial distribution [8]

$$\omega_j=\binom{p-p_a}{j}\left[\frac{Z}{A}\right]^j\left[\frac{N}{A}\right]^{p-p_a-j}. \tag{13}$$

B. Formation probability of clusters

The formation probability $K_n^{lm}(E_x)$ of Eq. (8) is obtained from the formalism of Refs. [4,5] with two modifications. Iwamoto and co-workers assume that the cluster nucleons are bound in a simple harmonic oscillator potential whose frequency ω_x is determined by the measured radius of the cluster. They take the formation probability $F_{lm}(E_x)$ to be proportional to the microstates available to the cluster

$$I_{lm}(E_x)=\frac{1}{h^{3(A_x-1)}}\prod_{i=1}^{A_x-1}\int \mathbf{dk}_i\int \mathbf{d}\xi_i, \tag{14}$$

$$F_{lm}(E_x)=\frac{I_{lm}(E_x)}{\Sigma_l I_{lm}(E_x)}, \tag{15}$$

where ξ_i and $\mathbf{k}_i$ are the A_x-1 relative coordinates and momenta, respectively, of the A_x nucleons.

The modifications introduced in the present work are as follows. First, in evaluating Eq. (14) Refs. [4,5] assume that the emitted cluster is formed at the surface of the nucleus. We do away with this restriction and evaluate the formation probability inside the nuclear volume using the limits for $\mathbf{k}_i$ and ξ_i of [7]. This considerably simplifies the evaluation of Eq. (14). The possibility of the cluster formed inside the nuclear volume dissolving into its constituents before reaching the surface can be taken into account while calculating the emission probability. Second, while Refs. [4,5,7] neglect the distinguishability of protons and neutrons and evaluate Eq. (14) for A_x identical nucleons, we introduce the distinguishability of protons and neutrons and write

$$K_n^{lm}(E_x)=R_n^{lm}(x)F_{lm}(E_x), \tag{16}$$

$$R_n^{lm}(x)=\sum_j w_j\sum_{\{x_{\pi l}\}} R(x_{\pi l},j), \tag{17}$$

where $R_n^{lm}(x)$ is the probability of choosing $x_{\pi l}$ protons and $x_{\nu l}$ neutrons from above the Fermi surface and $x_{\pi m}$ protons and $x_{\nu m}$ neutrons from below. The normalization of $K_n^{lm}(E_x)$ is the same as that of $F_{lm}(E_x)$ of Eq. (15) in the sense that if the constraint (6) is removed while summing over $\{x_{\pi l}\}$ in Eq. (17) we have $R_n^{lm}(x)=1$ and $K_n^{lm}(E_x)=F_{lm}(E_x)$.

C. Energy distribution of clusters

Before the cluster is formed in the n-exciton state, the excitation energy E_c is shared among p excited particles and h holes. After the cluster is formed with energy E_x, the energy $U=E_c-E_x$ is shared among $p-l$ excited particles and $h+m$ holes. The probability of transition from the initial (p,h) state to the $(p-l,h+m)$ plus cluster state is accounted for in the cluster formation probability.

Of the $n'=n-l+m$ excitons that share U, the energy e_1 of the first exciton varies between $0\leqslant e_1\leqslant U$, that of the second exciton between $0\leqslant e_2\leqslant U-e_1$, and so on until the energy $e_{n'-1}$ of the $n'-1$ exciton varies between $0\leqslant e_{n'-1}\leqslant U-\Sigma_{j=1}^{n'-2}e_j$. By conservation of energy U, the n' exciton then has a fixed energy $e_{n'}=U-\Sigma_{j=1}^{n'-1}e_j$. The density of states $\rho_n^{lm}(U,E_x)$, where the cluster has energy E_x and $n-l+m$ excitons share U, is determined by the convolution of the exciton state densities $\rho_1(e_1)$, $\rho_2(e_2)$, . . . , and the cluster density of states $\rho_x(E_x)$ integrated over the allowed values of exciton energies. Using the equidistant spacing model, $\rho_1(e_1)=\rho_2(e_2)=\cdots=g$, the nucleon single-particle level density, $\rho_x(E_x)=g_x$, and

$$\rho_n^{lm}(U,E_x)=\frac{(p-l)!}{p!}\frac{g_x g^{n'}}{(p-l)!(h+m)!}\left[\prod_{r=1}^{n'-1}\int_0^{U_r}de_r\right]$$
$$=\frac{g_x g(gU)^{n-l+m-1}}{p!(h+m)!(n-l+m-1)!}, \tag{18}$$

where the upper limit of the integrals are $U_r=U$ for $r=1$ and $U_r=U-\Sigma_{j=1}^{r-1}e_j$ for $r>1$. The factors $(p-l)!$ and $(h+m)!$ in the denominator of the first equality remove multiple counting of configurations arising from identical particles and holes. Also, since $p!/(p-l)!$ permutations are possible to select l identical excited particles and $\rho_n^{lm}(U,E_x)$ refers to only one such permutation, Eq. (18) has to be multiplied by its *a priori* probablity $p!/(p-l)!$.

Assuming as in the case of the standard hybrid model for nucleon emissions (5) that $P_n^{lm}(E_x)\propto\rho_n^{lm}(U,E_x)$, the proportionality constant is obtained from the normalization $\int_0^{E_c}P_n^{lm}(E_x)dE_x=1$, which conserves the number of clusters formed with given (l,m) in the n-exciton state. We then have

$$P_n^{lm}(E_x)=\frac{\rho_n^{lm}(U,E_x)}{\rho_n^{lm}(\text{total})},$$

$$\rho_n^{lm}(\text{total})=\frac{g_x(gE_c)^{n-l+m}}{p!(h+m)!(n-l+m)!}. \tag{19}$$

In Refs. [4,5] the participation of m holes in sharing U is neglected under the assumption that the m nucleons emerging as cluster constituents come out freely without interacting with the remaining nucleons. This assumption of $m=0$ in Eq. (18) is contrary to energy conservation since U is the sum of the excitation energies of particle and hole excitons. Neglecting the excitation of the m holes results in $U<E_c-E_x$.

III. NUMERICAL RESULTS

Using Eqs. (19) and (8) in Eq. (2) and combining with Eq. (1), the cluster emission spectrum in the extended hybrid model is

$$\sigma(\epsilon_x)=\sigma_{abs}\sum_{\substack{n=n_0\\ \Delta n=2}}^{\bar{n}} D_n\sum_{l=0}^{A_x} W_{nlm}(\epsilon_x)\tau_n(\epsilon_x), \tag{20}$$

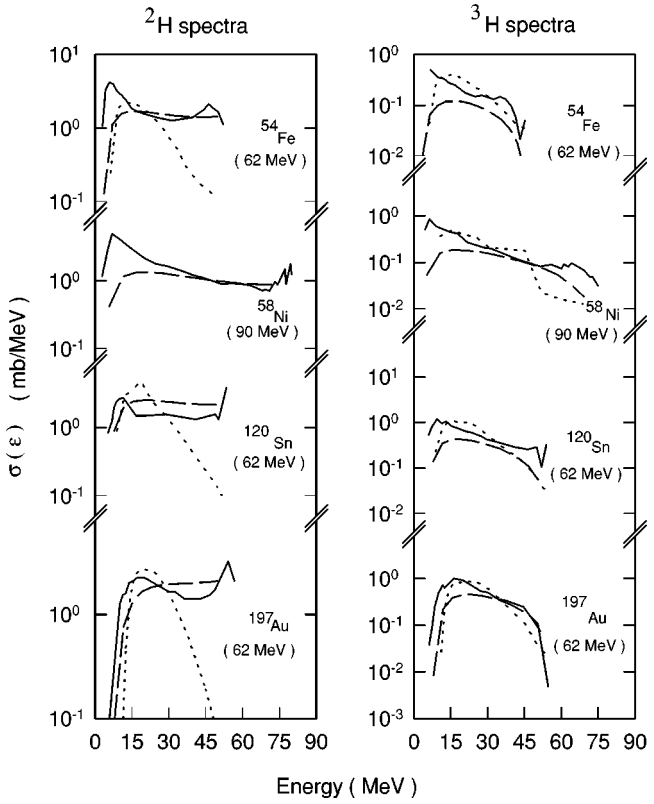

FIG. 1. Comparison of present calculations (dashed lines) with experimental spectra (full lines) and exciton model [5] predictions (dotted lines) for deuteron and triton spectra from proton-induced reactions. The targets and incident energies are marked against the spectra. The experimental data for ^{58}Ni are from [3] and others from [12].

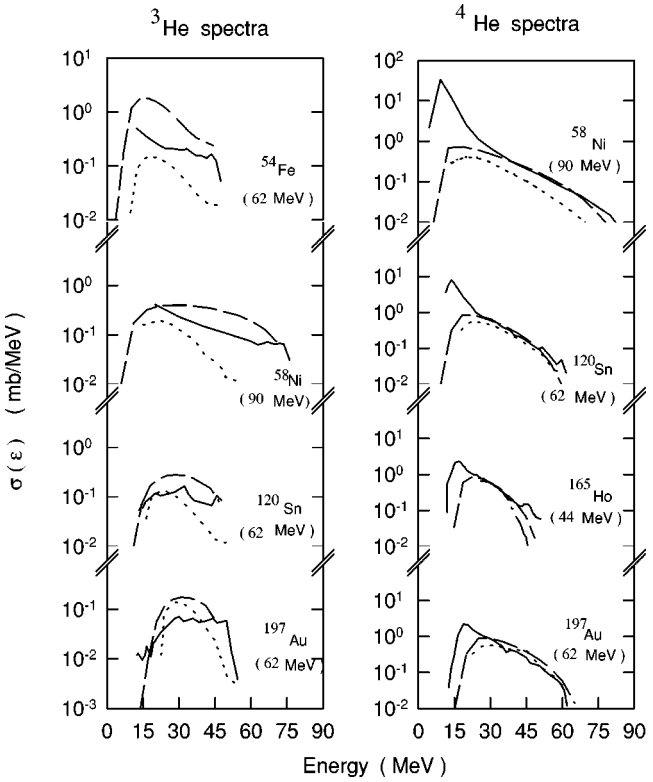

FIG. 2. Same as in Fig. 1, but for helion and α-particle model parameters. Experimental and FKK calculations (dashed-dot line) for ^{165}Ho are from [1].

with

$$W_{nlm}(\epsilon_x)=\left[N_n^{lm}(x)R_n^{lm}(x)F_{lm}(E_x)\frac{\rho_n^{lm}(U,E_x)}{\rho_n^{lm}(\text{total})}\right]\lambda_e(\epsilon_x), \tag{21}$$

where $\lambda_e(\epsilon_x)$ and $\tau_n(\epsilon_x)$ are given, respectively, by Eqs. (3) and (4). It should be noted that $F_{lm}(E_x)$ is evaluated inside the nuclear volume instead of at the nuclear surface, as is done in the case of exciton model calculations of Refs. [4,5]. The cluster formed inside the volume may dissolve into its constituents before reaching the surface. This depends on the cluster mean free path, which is inversely proportional to W. Since $\tau_n(\epsilon_x)$ of Eq. (4) takes into account the cluster-nucleon interaction rate $2W/\hbar$, the probability of the cluster dissolving into its constituents is included in the emission probability $W_n(\epsilon_x)\tau_n(\epsilon_x)$. Thus, in the framework of the hybrid model, the evaluation of cluster formation probability is greatly simplified by removing the surface restrictions. In the exciton model, on the other hand, the emission probability does not include competitions from cluster-nucleon interactions but only nucleon-nucleon interactions [shown later in Eq. (23) and discussed in the following] and it becomes necessary to calculate the formation probability at the nuclear surface. In the case of PEQ nucleon emissions, $N_n^{lm}(x)$ is the number of excited protons or neutrons [X_n^x of Eq. (5)], $K_n^{lm}(E_x)=1$, $l=1$, $m=0$, and Eqs. (20) and (21) reduce to the standard hybrid model expressions.

The formalism is tested for several proton-induced reactions shown in Figs. 1 and 2, where the present calculations for PEQ emissions are compared with experiment, the previous exciton model, and FKK theory calculations. The calculations are performed with $g=A/13$, $g_x=g/A_x$, $\epsilon_F=33.5$ MeV, and ω_x from Ref. [5]. The proton, deuteron, and α-particle optical model parameters are from Refs. [6,9,10], respectively, and the triton and helion parameters are from Ref. [11]. For nucleon-induced reactions the initial configuration is a $2p$-$1h$ state with $n_0=3$. Since no attempt is made to reproduce the equilibrium or near-equilibrium part of the spectra, we have restricted our calculations to $\overline{n=7}$ ($4p$-$3h$) as larger particle-hole configurations contribute negligibly to the high-energy part of the spectra. D_n of Eq. (20) is evaluated as in Ref. [6], with PEQ emissions restricted to those of single nucleons.

The present calculations show remarkable improvements in predicting deuteron spectra. Significant changes also occur in α spectra compared to the exciton model calculations for ^{58}Ni and FKK theory for ^{165}Ho. The triton spectra are well reproduced by both the exciton model and the present calculations with the latter reproducing the trend better for ^{54}Fe and ^{120}Sn, although the observed spectra are underpredicted. The predicted helion spectra, however, overcorrect the underpredictions of the exciton model; adjustment of the helion optical model parameters, which determine both the decay rate $\lambda_e(\epsilon_x)$ and the lifetime $\tau_n(\epsilon_x)$, may lead to better agreement.

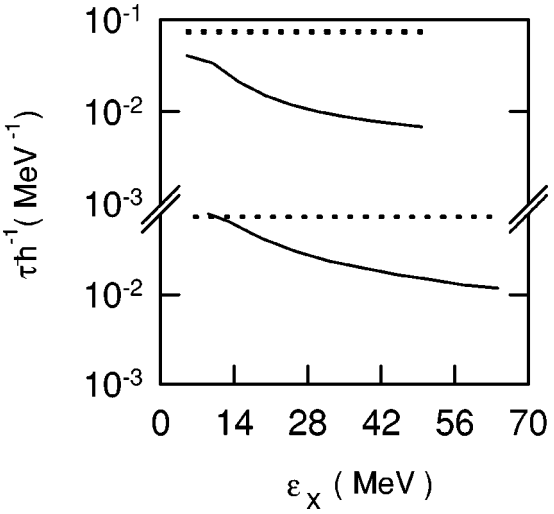

FIG. 3. Comparison of the lifetimes of the exciton (dotted lines) and the hybrid (full lines) models for (a) deuteron emissions from ^{54}Fe+p and (b) α-particle emissions from ^{120}Sn+p, both at 62 MeV proton energy. The exciton model lifetimes for $n=3,5,7$ are too close to be shown separately.

IV. DISCUSSION

The crucial importance of the preemission cluster energy distribution in predicting the emitted cluster spectra can be seen through a comparison of the ingredients of the hybrid and exciton models. Although the closed-form exciton model cross section can be written as in Eq. (1), the emission rate $W_n^{(E)}(\epsilon_x)$ and the mean lifetime $\tau_n^{(E)}(\epsilon_x)$ [the superscript (E) refers to exciton model variables] are evaluated from different physical conditions.

For nucleon emissions, $W_n^{(E)}(\epsilon_x)$ is obtained from the principle of detailed balance with $\rho_n(E_c)$ as the initial-state density and the final-state density as the product of the state density $\rho_{n_r}(U)$ of the residual nucleus and the number of states available to the ejectile from its translational motion

$$W_n^{(E)}(\epsilon_x)=\frac{(2s_x+1)\mu_x\epsilon_x\sigma_{inv}(\epsilon_x)}{\pi^2\hbar^3}\frac{\rho_{n_r}(U)}{\rho_n(E_c)}, \qquad (22)$$

where n_r $(=n-1)$ is the exciton number of the residual nucleus. This expression is different from the corresponding hybrid model $W_n(\epsilon_x)$ of Eq. (2). First, Eq. (22) is the emission rate from the n-exciton state as a whole, while Eq. (2) evaluates the emission rate from a particular configuration of the n-exciton state through a two-step process: the excitation of the ejectile inside the mother nucleus to energy E_x followed by its emission with energy ϵ_x. Second, the energy dependence in Eq. (22) is determined entirely by postemission conditions because the exciton model assumes that all configurations of the n-exciton state occur with equal *a priori* probability. The hybrid model, on the other hand, uses both pre- and postemission conditions to evaluate $W_n(\epsilon_x)$. The former is taken into account in defining $f_n^x(E_x)$ in Eq. (2) through $P_n(E_x)$ of Eq. (5) [or $f_{nlm}^x(E_x)$ of Eq. (8) and $P_n^{lm}(E_x)$ of Eq. (19) for clusters] and the latter through Eq. (3), where the postemission ejectile energy determines the decay rate.

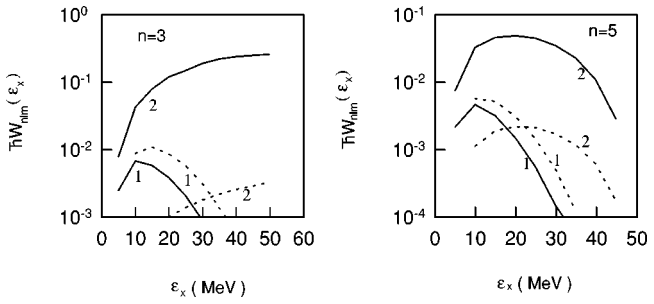

FIG. 4. Deuteron emission rates from ^{54}Fe+p at 62 MeV incident energy from $n=3$ and 5. The dotted and full lines are those of the exciton and hybrid models, respectively. The values of l are shown against individual curves.

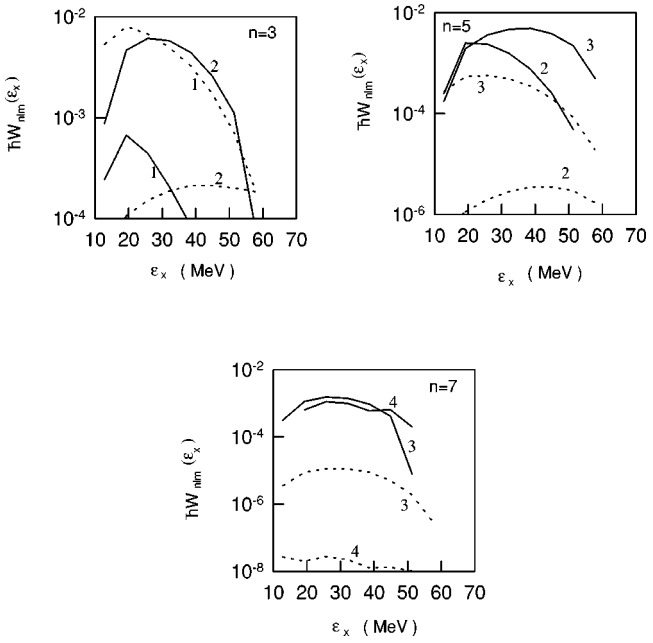

FIG. 5. Same as in Fig. 4, but for α-particle emissions from ^{120}Sn+p at 62 MeV from $n=3$, 5, and 7.

The mean lifetime $\tau_n^{(E)}(\epsilon_x)$ is written as

$$\tau_n^{(E)}(\epsilon_x)=\frac{1}{\Sigma_x\int_0^{E_c}W_n^{(E)}(\epsilon_x)dE_x+\lambda_{total}^n}, \qquad (23)$$

where λ_{total}^n is the sum of the nucleon-nucleon interaction rates that result in $\Delta n=\pm 2,0$ transitions. Equation (23) is the mean lifetime of the n exciton as a whole since it takes into account decays of all possible types of ejectiles with all possible energies as well as $\Delta n=\pm 2,0$ transitions. This is in contrast to Eq. (4), where only the decay of the ejectile of interest and its two-body interaction rate with other particles are considered making it the lifetime of that configuration of the n-exciton state from which the decay occurs.

References [4,5] extend the exciton model to cluster emissions by writing $W_n^{(E)}(\epsilon_x)=\Sigma_l W_{nlm}^{(E)}(\epsilon_x)$, where $W_{nlm}^{(E)}(\epsilon_x)$ is obtained by multiplying Eq. (22) by $F_{lm}(E_x)$ and setting $n_r=n-l$. In order to compare in detail the effects of preemission energy distributions with those of the exciton model, we rearrange the terms of $W_{nlm}^{(E)}(\epsilon_x)$ and write

$$W_{nlm}^{(E)}=\left[\frac{p!}{(p-l)!}F_{lm}(E_x)\frac{\rho_n^{l0}(U,E_x)}{\rho_n(E_c)}\right]\lambda_e(\epsilon_x) \qquad (24)$$

in terms of the hybrid model decay $\lambda_e(\epsilon_x)$. The factor inside the square brackets is the cluster energy distribution as calculated from postemission conditions for given l and m. $\rho_n^{l0}(U,E_x)$ is evaluated from Eq. (18) with $m=0$ and $\rho_n(E_c)$ from Eq. (19) with $g_x=g$, $l=1$, and $m=0$.

As is evident from Eqs. (4) and (23), $\tau_n^{(E)}(\epsilon_x)$, in contrast to $\tau_n(\epsilon_x)$, is independent of the type of ejectile and its energy; it is constant for a given n. A comparison of $\tau_n^{(E)}(\epsilon_x)$ and $\tau_n(\epsilon_x)$ in Fig. 3 shows that the latter decreases by as much as an order of magnitude for higher ϵ_x.

Yet, even with much smaller lifetimes, the present calculations predict cross sections that are comparable to the exciton model calculations for the triton and α particle and much larger for deuteron and helion (Figs. 1 and 2). This is because of the difference in the emission rates (21) and (24) shown in Figs. 4 and 5. More particularly, the difference arises from the phase-space ratios $\rho_n^{lm}(U,E_x)/\rho_n^{lm}(\text{total})$ of Eq. (21) and $\rho_n^{l0}/\rho_n(E_c)$ of Eq. (24) that determine the preemission cluster energy distributions in the two models.

It can be seen from Fig. 4 that the high-energy deuterons are predominantly emitted from $n=3$ with $l=2$, $m=0$. In this case $\rho_n^{l0}(U,E_x)$ of Eq. (21) is the same as $\rho_n^{lm}(U,E_x)$ of Eq. (24), but $\rho_n(E_c)$ of Eq. (24) is much larger than $\rho_n^{20}(\text{total})$ of Eq. (21). Consequently, $W_{nlm}^{(E)}(\epsilon_x)$ is about two orders of magnitude less than $W_{nlm}(\epsilon_x)$ for higher values of ϵ_x (for $n=3$). With $\tau_n(\epsilon_x)$, on the other hand, about an order of magnitude less than $\tau_n^{(E)}(\epsilon_x)$ (Fig. 3), the emission probability (the product of emission rate and lifetime) is about an order of magnitude larger in the present calculations.

In the case of α-particle emission, significant contributions to higher energies occur for $m>0$, viz., $l=1$, $m=3$ and $l=2$, $m=2$ from $n=3$; $l=2$, $m=2$ and $l=3$, $m=1$ from $n=5$; and $l=3$, $m=1$ and $l=4$, $m=0$ from $n=7$. As is evident from Fig. 5, the total emission rates from $n=3$ are about the same in both models. But for $n=5$ and 7, $W_{nlm}(\epsilon_x)$ is much larger than $W_{nlm}^{(E)}(\epsilon_x)$ for higher ϵ_x. This results from the fact that in the exciton model $\rho_n^{l0}(U,E_x)$ decreases with increasing l with $\rho_n(E_c)$ remaining constant, while in the present calculations both $\rho_n^{lm}(U,E_x)$ and $\rho_n^{lm}(\text{total})$ decrease with increasing l. However, the larger values of $W_{nlm}(\epsilon_x)$ are compensated by the smaller values of $\tau_n(\epsilon_x)$ and both calculations give comparable agreement with experiment.

It should be noted that the ansatz of $m=0$ of Refs. [4,5] is unphysical as it violates energy conservation. If the role of m is included, as it should be, in defining the residual phase space, then the exciton model α-particle spectrum will give large overpredictions. The inclusion of m, however, will have a negligible effect on the high-energy part of the exciton model deuteron spectrum since these emissions occur primarily with $l=2,m=0$.

[1] H. B. Olaniyi, P. Demetriou, and P. E. Hodgson, J. Phys. G **21**, 361 (1995).

[2] J. Bisplinghoff, Phys. Rev. C **50**, 1611 (1994).

[3] J. R. Wu and C. C. Chang, Phys. Rev. C **17**, 1540 (1978).

[4] A. Iwamoto and K. Harada, Phys. Rev. C **26**, 1821 (1982).

[5] K. Sato, A. Iwamoto, and K. Harada, Phys. Rev. C **28**, 1527 (1983).

[6] M. Blann and H. Vonach, Phys. Rev. C **28**, 1475 (1983).

[7] Z. Jingshang, Y. Shiwei, and W. Cuilan, Z. Phys. A **344**, 251 (1993).

[8] C. K. Cline, Nucl. Phys. **A193**, 417 (1972).

[9] W. W. Daehnick, J. D. Childs, and Z. Vrcelj, Phys. Rev. C **21**, 2253 (1980).

[10] V. Avrigeanu, P. E. Hodgson, and M. Avrigeanu, Phys. Rev. C **49**, 2136 (1994).

[11] F. D. Becchetti and G. W. Greenless, in *Proceedings of the Third International Symposium on Polarization Phenomena in Nuclear Reactions, Madison, 1975*, edited by H. H. Barshall and W. Haeberli (University of Wisconsin Press, Madison, 1971), p. 682.

[12] F. E. Bertrand and R. W. Peelle, Phys. Rev. C **8**, 1045 (1973).